



Mobilization Study of the Capillarity-Induced Resonance of Blobs in a Converging-Diverging Duct

Pitambar Randive¹ and Amaresh Dalal^{2*}

¹Department of Mechanical Engineering, National Institute of Technology Silchar,
Silchar-781 029, India
Email: kp691975@gmail.com

²Department of Mechanical Engineering, Indian Institute of Technology Guwahati,
Guwahati-781 039, India
Email: amaresh@iitg.ernet.in

*Corresponding author: Email: amaresh@iitg.ernet.in, Tel.: +91-361-2582677

Abstract

It is well known from experiments and theoretical considerations that the blobs in capillary tubes are subjected to resonance due to entrapment owing to interfacial tension. The present work deals with the study of the capillarity induced resonance which can mobilize the trapped blobs when excited at the resonant frequency. Mesoscopic approach of lattice Boltzmann method is used to understand the response of blobs having pinned menisci in convergent-divergent duct to an oscillatory force. The mobilization of the trapped non-wetting phase blobs due to capillarity-wettability interaction is analyzed. It has been observed that the movement of the blob was found to be relatively slower on the surfaces with mixed wettability as compared to the uniform wetted surface. The results obtained could be very useful in the fields like recovery of oil to provide a quantitative tool for estimating the parameters required to liberate entrapped non-wetting fluid.

Keywords: *Wettability, blob dynamics, lattice Boltzmann method*

1. Introduction

In the recent past, an upsurge of interest among researchers in the field of enhanced oil recovery has been witnessed. The main issue in this context is to reduce the amount of oil entrapped and to mobilize it. However, it is not possible to mobilize the trapped blobs by an imposed flow in the surrounding connected fluid phase without changing fluid properties. The mobilization of the trapped oil blob by vibrations and elastic waves is one of the potential methods of enhanced petroleum recovery (Beresnev and Johnson (1994); Roberts et al. (2003)). In this context, Hilpert et al. (1999) proposed the model to explain the effect of forces on trapped blob and its mobilization. They explained the dynamics of the three-phase contact. This contact line remains either pinned on heterogeneities of the boundary surface or slide if oscillating body force is applied. It was hypothesized by Hilpert et al. (2000) that the trapped oil blobs exhibit meniscus resonance similar to the liquid column trapped in a capillary tube. They further stated that pinned contact lines can be found for oscillatory flows and vibrations of the solid surface as well. They explored the mobilization of the trapped blob with the help of sound waves at their resonance frequencies which could induce such large oscillations of the trapped oil blobs generally referred to as "capillarity induced resonance". This in turn, could help the blob to reach unstable position and pass the constrictions of the pore space. They argued that this capillarity induced resonance is very useful to mobilize the trapped blob which can enhance oil recovery.

The pioneering work investigating the transport of blob was carried out by Ng et al. (1978) who performed experiments to visualize the displacement behavior of blob. Later on, Larson et al. (1981) opined that the capillary number needed to induce motion in a trapped blob increases with the decrease in the length of blob along direction of the pressure gradient. Mason (1983) proposed model for the trapped oil blobs with a random packing of spheres. Yadav and Mason (1983) studied the motion of blob passing through a sphere packing and calculated the probability of blob motion. Wang and Dong (2011) analysed the imbibition of trapped oil with interacting serial type triangular tube bundle models. They found that the residual oil saturation for different viscosity ratios to be a function of capillary number. Soares et al. (2005) investigated the displacement of liquid in capillary tubes at different operating parameters.

Many researchers worked in the area of propagation of sound saturated with multiple immiscible fluids (Palmer and Traviolia (1980); Mavko and Nur (1979); Santos et al. (1990); Tuncay. and Corapcioglu (1996); Murphy (1982); Karapetsas et al. (2013, 2014)). However, they could not provide expressions for the resonances. Graham and Higdon (2000) showed that droplet deformation owing to oscillatory force can result to increase in average flow rate for flow through the capillary tubes. Beresnev and Johnson (1994) reviewed the influence of elastic waves and reported that its application on subsurface actually increases the efficiency of water flooding of oil reservoirs (Roberts et al. (2003); Kostrov et al. (2001)). The major obstacle in extraction of oil basically the large velocities needed to recover the nonwetting phase blobs (Hunt et al. (1988); Dias and Payatakes (1986)). Iassonov and Beresnev (2003) reported the influence of sonic vibrations with low frequency on the flow of non-aqueous phase liquids (NAPL) through a porous medium. It is argued that yield stress rheology of the fluid in pore and trapping due to capillary generates the same behavior at the macroscopic level. This is of utmost importance to understand the mobilization of reservoir fluids with the vibration stimulus. Vibrations can considerably reduce minimum pressure gradient needed to mobilize entrapped fluid and to increase the mean mass flow rate. Vibrations are the most effective in the regions of relatively less pressure gradients. Palan et al. (2006) applied the vibrio-acoustics method so as to drain water required to form droplet for the given input excitation frequency and amplitude. Numerical simulation approach has been used widely to explore the dynamics of immiscible fluid flow by several investigators (Lauga and Stone (2003); He and Kasagi (2008); Davies et al. (2006); Adroher and Wang (2011)).

In recent past, lattice Boltzmann (LB) method was extensively used for detailed insight of the underlying physics of immiscible flows (Inamuro (2006); Shina and Kima (2013)). In particular, Shan and Chen (S-C) model (Kang et al. (2005)) has been employed to explore the contact line mechanisms, mainly due to its approach which considers interaction. Zhang and Kwok (2004) analysed the wetting phenomenon which studies the motion of a contact line in between two super hydrophobic surfaces with the help of free energy model. Briant et al. (2004) also used LB method to simulate motion of contact line in liquid-gas systems as well as binary fluids. Kang et al. (2010) gave an excellent overview on the recent developments on LBM modeling of transport phenomena for porous media.

Recently, Hilpert (2007); Yiotis et al. (2010, 2013) used lattice Boltzmann (LB) modeling to simulate the blob behavior. Yiotis et al. (2013) studied the dynamics of nonwetting blobs and discussed the mechanism of breaking up as well as blob coalescence. However, the mechanism of mobilization is entirely different, when it is a case of changing cross-sectional area. For instance, the movement is more for the sinusoidal pore ducts as compared to the disc packing (Hilpert (2007)). In spite of these efforts, mechanism of capillarity induced resonance and its influence on mobilization of the blob for the surface with varied wettability configurations is not known properly. This motivates us to gain more insight into capillarity-wettability interaction in conjunction with capillarity induced resonance.

2. Problem specification

The main focus of the present work is to investigate the resonance in case of fluid configurations having two menisci and to derive the frequency response of a blob trapped in a converging-diverging channel of radius (R) (see Fig. 1 (a)). In this work, the applied body force mimics the acoustic excitation and is used to study the displacement of blob. The breadth, length and width of the domain as shown in Fig. 1 (b) used for the study are 100 (l_z), 48 (l_x) and 48 (l_y) (in lattice units), respectively. Length of nonwetting and wetting phase is given by L_w and L_n , respectively. Shan and Chen model is considered here for the system having two immiscible fluids. The domain consists of displacing fluid (fluid 1) with a trapped blob (fluid 2). The blob is initially located at the center of the domain i.e., $z = 50$. The motion of the blob is achieved by transient force in the z -direction. The dynamic behavior of the blob is explored for the parameters like frequency applied, wettability and thickness of the blob. The periodic boundary condition is considered in z -direction and no slip boundary condition is taken at the walls in x - and y -direction. The location of interface is considered at the midsection along x axis at which both the fluid have equal number density (Kang et al. (2005)).

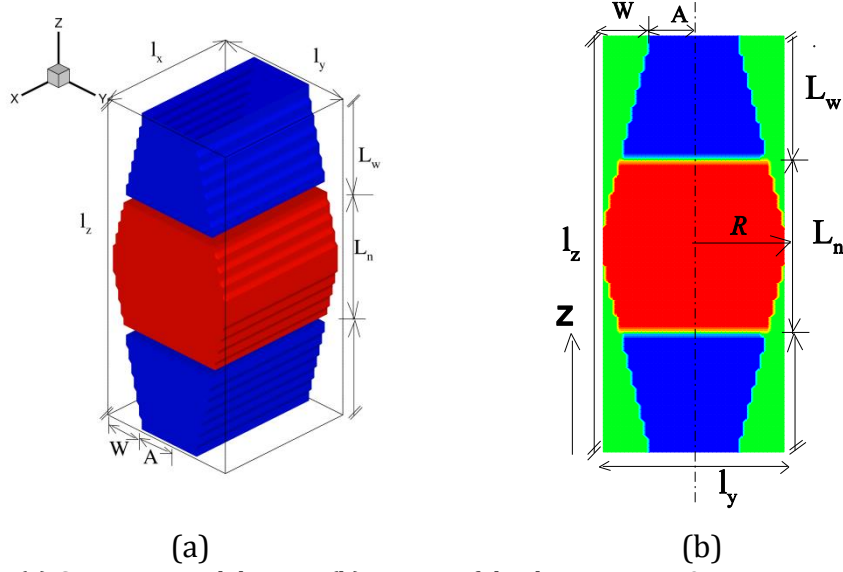


Figure 1: (a) Computational domain, (b) section of the domain at $x = 24$.

3. Formulation: lattice Boltzmann model

The lattice Boltzmann method has been extensively applied to predict the behavior of multiphase fluid flows in recent past mainly for the applications dealing complex geometries and the interfacial dynamics (Raabe (2004); Chen and Doolen (1998)). He et al. (1999) proposed a novel model based on kinetic equation. Gunstensen et al. (1991) developed a model which is inspired from a two-component lattice gas model. Swift et al. (1995) worked with free energy approach for lattice Boltzmann model. However, S-C model (Shan et al. (1993)) is employed for the simulation in the present work because it takes into account the interaction of neighboring particles in the form of interaction potential for multiphase flow. It also satisfies Galilean invariance (Shan and Doolen (1995)). It may be noted that it is not required to track the interface while simulating the motion of the immiscible droplet using this model. Moreover, it is very convenient in handling fluid/solid interaction. The brief formulation of LBM is discussed below. Each fluid component is represented by a distribution function. The lattice Boltzmann equations for the k^{th} component can be expressed in the form given below:

$$f_i^k(\mathbf{x} + \mathbf{c}_i \delta_t, t + \delta_t) - f_i^k(\mathbf{x}, t) = \frac{f_i^k(\mathbf{x}, t) - f_i^{k(eq)}(\mathbf{x}, t)}{\tau_k} \quad (1)$$

where $f_i^k(\mathbf{x}, t)$ is the number density distribution function for the k^{th} component in the i^{th} velocity direction at position \mathbf{x} and time t . \mathbf{c}_i is the discrete velocity and δ_t is the time increment. The relaxation time of the k^{th} component is given as τ_k whereas $f_i^{k(eq)}(\mathbf{x}, t)$ indicates the corresponding equilibrium distribution function. $f_i^{k(eq)}(\mathbf{x}, t)$ for $D3Q19$ model (refer Fig. 2 where D and Q represent the dimension and the number of velocity directions) has the following form.

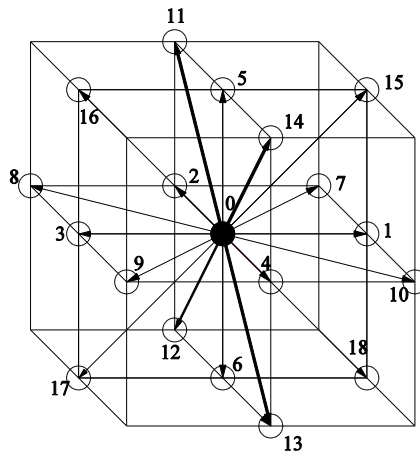


Figure 2: D3Q19 lattice structure schematic.

$$f_i^{k(eq)} = d_k n_k - \frac{1}{2} n_k \mathbf{u}_k^{eq} \mathbf{u}_k^{eq} \quad \text{for } i = 0 \quad (2)$$

$$f_i^{k(eq)} = \frac{1-d_k}{12} n_k + \frac{1}{6} n_k (\mathbf{c}_i \cdot \mathbf{u}_k^{eq}) + \frac{1}{4} n_k (\mathbf{c}_i \cdot \mathbf{u}_k^{eq})^2 - \frac{1}{12} n_k \mathbf{u}_k^{eq} \mathbf{u}_k^{eq} \quad \text{for } i = 1, 2, 3, \dots, 6 \quad (3)$$

$$f_i^{k(eq)} = \frac{1-d_k}{24} n_k + \frac{1}{12} n_k (\mathbf{c}_i \cdot \mathbf{u}_k^{eq}) + \frac{1}{8} n_k (\mathbf{c}_i \cdot \mathbf{u}_k^{eq})^2 - \frac{1}{24} n_k (\mathbf{u}_k^{eq} \mathbf{u}_k^{eq}) \quad \text{for } i = 7, 8, 9, \dots, 18 \quad (4)$$

$$\text{where } \mathbf{c}_i = (0, 0, 0) \quad \text{for } i = 0 \quad (5)$$

$$\mathbf{c}_i = (\pm 1, 0, 0), (0, \pm 1, 0), (0, 0, \pm 1) \quad \text{for } i = 1-6$$

$$\mathbf{c}_i = (\pm 1, \pm 1, 0), (\pm 1, 0, \pm 1), (0, \pm 1, \pm 1) \quad \text{for } i = 7-18$$

$$(c_s^k)^2 = \frac{1-d_k}{2} \quad (6)$$

Where, d_k is a free parameter related to speed of sound c_s^k of pure k^{th} component. The properties like velocity and density are obtained by taking the moments of the distribution function as follows.

$$n_k = \sum_i f_i^k \quad (7)$$

Where, n_k is the number density of k^{th} component. The density and velocity of each component are given as below.

$$\rho_k = m_k n_k = m_k \sum_i f_i^k \quad (8)$$

Where, m_k is mass of k^{th} component.

$$\rho_k \mathbf{u}_k = m_k \sum_i \mathbf{c}_i f_i^k \quad (9)$$

The kinematic viscosity in lattice unit is

$$\nu_k = (\tau_k - 1/2)(c_s^k)^2 \quad (10)$$

Interaction force includes an altered velocity in the equilibrium distribution function. The momentum taking into account the interaction force is given by \mathbf{u}_k^{eq}

$$\rho_k \mathbf{u}_k^{eq} = \rho_k \mathbf{u}' + \tau_k \mathbf{F}_k \quad (11)$$

It may be noted that \mathbf{u}_k^{eq} is used to calculate the density distribution function (refer Eqs. (2) - (3)), where \mathbf{u}' is an additional component on the top to account for interparticle interaction for each component. Net force acting on the k^{th} component is given by \mathbf{F}_k which includes fluid/fluid interaction \mathbf{F}_{1k} , fluid/solid interaction \mathbf{F}_{2k} , and external force \mathbf{F}_{3k} (Martys and Chen (1996)) and is given as

$$\mathbf{F}_k = \mathbf{F}_{1k} + \mathbf{F}_{2k} + \mathbf{F}_{3k} \quad (12)$$

It may be noted that the continuity and momentum equations can be expressed for the mixture of fluid as a single fluid with Chapman-Enskog expansion in the incompressible limit (Shan and Doolen (1996)). Here, net density and velocity of the fluid mixture can be calculated, respectively, by Shan and Doolen (1995)

$$\rho = \sum_k m_k \sum_i f_i^k \quad (13)$$

$$\rho \mathbf{u} = \sum_k m_k \rho_k \mathbf{u}_k + \frac{1}{2} \sum_k \mathbf{F}_k \quad (14)$$

The details of S-C models can be found from Kang et al. (2002, 2005); Randive and Dalal (2013). It may be noted that for the present work, the interface is taken at the location where both the fluids have same number density. The evaluations of fluid/solid and fluid/fluid interaction parameters are required to calibrate the model. In this context, two numerical tests have been performed on the similar line as that of Mukherjee et al. (2009) namely static droplet and bubble test. Bubble test is carried out in the absence of solid phase to calculate the fluid/fluid interaction parameter and static droplet test is performed in the presence of solid wall to evaluate the fluid/solid interaction parameter. The interaction force \mathbf{F}_{1k} between the particles of k^{th} component at location \mathbf{x} and k^{th} component at location \mathbf{x}' is given as below.

$$F_{1k}(\mathbf{x}) = -\psi_k(\mathbf{x}) \sum_{\mathbf{x}'} \sum_{k=1}^s G_{kk}^-(\mathbf{x}, \mathbf{x}') \psi_k(\mathbf{x}') (\mathbf{x}' - \mathbf{x}) \quad (15)$$

where $\psi(\rho_k)$ and $G_{k\bar{k}}(\mathbf{x}, \mathbf{x}')$ is called as effective mass and Green's function, respectively. By varying the value of $G_{k\bar{k}}$, the surface tension force between the fluids can be regulated. The large value of $G_{k\bar{k}}$ results into separation of two mixed fluids (Martys and Chen (1996)) forming the well-defined interface. Bubble test is performed and value of surface tension is found to be 0.08. The static contact angle (Martys and Chen (1996); Kang et al. (2005); Mukherjee et al. (2009)) given by Eq. (16) which quantifies the force of interaction between the wall and fluid (Shan and Doolen (1996)) and is expressed as

$$F_{2k}(\mathbf{x}) = -n_k(\mathbf{x}) \sum_{\mathbf{x}'} g_{kw} n_w(\mathbf{x}') (\mathbf{x}' - \mathbf{x}) \quad (16)$$

where n_w is the number density of the wall and is constant at the wall and zero otherwise; whereas g_{kw} indicates interactive strength between the component k and the wall. The solid/fluid interaction parameter (g_{kw}) for the two-phase S-C LB model governs the influence of surface wettability which is manifested in terms of the contact angle at the solid/fluid/fluid interface. The static droplet test is conducted in the presence of a wall. The detailed procedure of this test is described in Mukherjee et al. (2009). Once static droplet is formed, estimation of the contact angle is done using the height a_0 , wetted length of the droplet b_0 and the final droplet radius R (Dullien (1992)) as shown in Fig. 3(a).

$$\tan(\theta_2) = \frac{b_0}{2(R - a_0)} \quad (17)$$

The final radius R , is given as

$$R = \frac{a_0}{2} + \frac{b_0^2}{8} \quad (18)$$

Figure 3 (a) shows θ_1 and θ_2 as the contact angles of fluids 1 and 2, respectively. The values of g_{1w} and g_{2w} are varied to get static droplets with varying contact angles. The value of $g_{2w} < 0$ gives a hydrophilic surface whereas $g_{2w} > 0$ leads to a hydrophobic surface as shown by static droplet test (Mukherjee et al. (2009)).

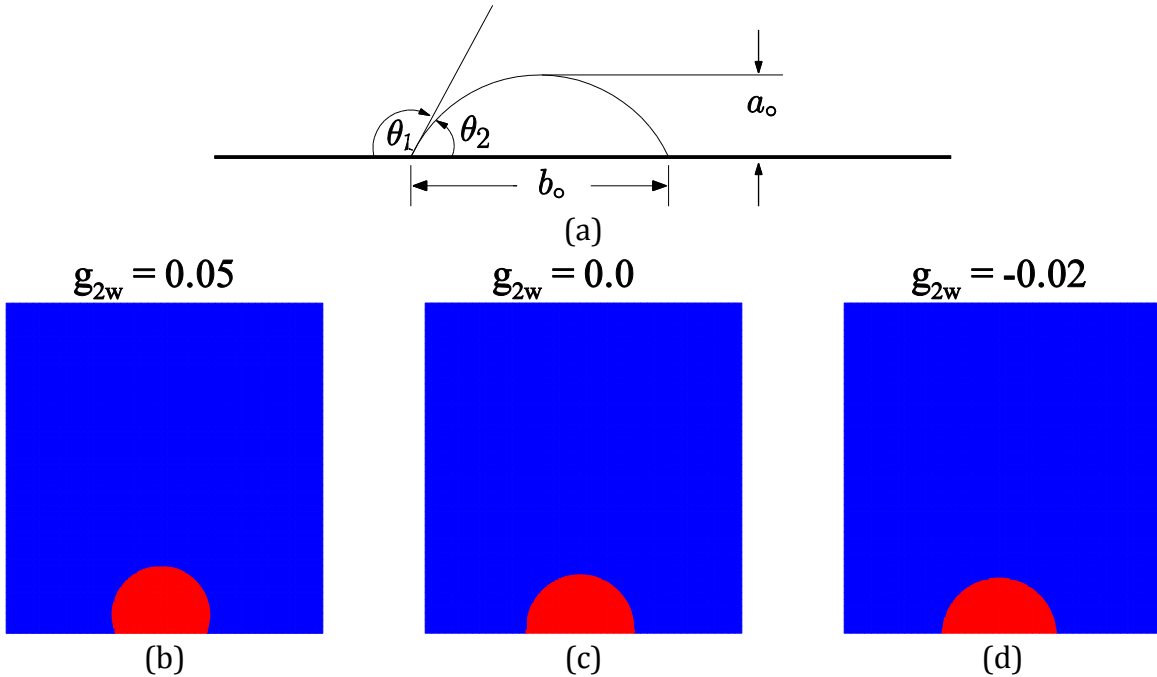


Figure 3: (a) Static droplet, (b) $\theta = 118^\circ$ for $g_{2w} = 0.05$, (c) $\theta = 90^\circ$ for $g_{2w} = 0.0$, (d) $\theta = 78^\circ$ for $g_{2w} = -0.02$.

4. Results and discussion

Enhanced oil recovery uses the methods like steam, gas and water flooding; explosive and hydraulic fracturing; injection of surfactants etc.. However, these methods have many limitations with some undesirable side effects. For instance, some methods are costly and need closing down the production and may result in detrimental consequences especially as far as the ecological balance is concerned. These impediments have forced engineers and geophysicists to look for new methods of stimulation. One such method is elastic wave stimulation which is not as a replacement for conventional EOR techniques, but as an alternative or complimentary tool which, in

certain situations, may make conventional methods more efficient. In this context, the mobilization of the trapped blob is systematically investigated. In this context, the blob dynamics is evaluated to understand the effect of capillarity-wettability interaction.

4.1. Dynamic behavior of the trapped nonwetting phase blob

LB simulations are carried out to investigate whether the model is able to capture the resonance of trapped non wetting phase blobs. It may be noted that a phase is said to be trapped in case no continuous path of that phase leads to the outlet. This path generally channels through spreading layers (i.e, through wetting layers) at the corners of the pores or through the centers of the pore space. The trapping of the blob is observed whenever meniscus is 'pinned' because of surface irregularities such as roughness on walls or chemical impurities (Hilpert (2007)). It needs the application of finite force to slide over the contact line (Hilpert et al. (2000); Leger and Joanny (1992); de Gennes (1985)). Pinning of the interface results in variation of the curvature of the oil/water interfaces at the corners as the applied pressure increases. As a consequence, the contact line does not get displaced. Instead, it keeps adjusting the curvature radius at the surface. In the present work, it is presumed that the contact line between the surface and fluid remains pinned to surface. Modelling of the surface roughness is done by adding solid phase pixels on both sides of the duct at two selected sites where three-phase contact point could be pinned (Hilpert (2007)). Roughness height is taken small so that it does not have significant impact on the flow in the channel but will be sufficient to 'trap' the contact line (Iassonov and Beresnev (2003)).

The blob is subject to the force \mathbf{F}_{3k} in z-direction as given below.

$$\mathbf{F}_{3k} = f(0) + \delta f(t) \quad (19)$$

where $f(0)$ and $\delta f(t)$ are body force and the perturbation, respectively. $f(0)$ can be considered equivalent to pressure gradient and to be imposed on the wetting phase (Hilpert (2007)) whereas the perturbation $\delta f(t)$ can be taken as a vibration of the walls. Thus, a capillarity induced resonance can be used to move the trapped blob by acoustic waves. The blob equilibrium contact angles at the bottom and top menisci are given θ_0^+ and θ_0^- , respectively. First of all, the non-wetting phase blob is initialized for a converging-diverging channel and equilibrium is reached through simulation. The fluid properties used in the present work are as given in Table 1.

Table 1: Parameter values for all numerical simulations

Parameter	Values (in lattice units)
Length of the channel (l_z)	100
Breadth (h)	48
Width (w)	48
Surface tension	0.08
Relaxation time of the wetting phase (τ_1)	0.80
Relaxation time of the nonwetting phase (τ_2)	0.80
Fluid-fluid interaction parameter	$g_{11} = g_{22}=0, g_{12} = g_{21}= 0.1$

Bounce back boundary conditions are applied at walls whereas periodic conditions are applied along the channel axis at $z = 1$ and $z = 0$. The periodic boundary condition connects the non-wetting phase over the outlet and inlet of the duct. The simulations are run on similar lines as that of by Hilpert (2007). Figure 1(b) indicates the distance between the wetting (L_n) and nonwetting phase L_w from three phase contact point. It may be noted that estimation of the viscous pressure drop for converging-diverging geometry is more complicated than that of a regular channel. Hilpert (2007) proposed an analytical model for the channels with varying cross-sectional area. The radius of the pore channel changes according to Eq. (20).

$$R(z) = \begin{cases} l_y/2 + 2A(z - l_z/2)/l_z & \text{for } 0 < z < l_z/2 \\ l_y/2 - 2A(z - l_z/2)/l_z & \text{for } l_z/2 < z < l_z \end{cases} \quad (20)$$

where $A = l_y/2$ represents width (w) whereas l_y indicates length in y -direction. In the characteristic frequency (see Eq. (24)), for the converging-diverging channel, variable size is taken into consideration to define mean radius by taking its average over the regions occupied by both the fluids Eq. (21).

$$\bar{R}(z) = \frac{1}{L_n} \int R(z) dz \quad (21)$$

Resonating frequency ω_0 can then be found using equation (Hilpert (2007)) given below.

$$\omega_0 = \sqrt{\frac{2\gamma(g(\theta_0^+) + g(\theta_0^-))}{(L_n\rho_n + L_w\rho_w)\bar{R}^2}} \quad (22)$$

where

$$g(\theta_0) = \sin\theta \left(2 - \frac{\pi - 2\theta - \sin(2\theta)\sin(2\theta)}{2\cos^4\theta} \right)^{-1} \quad (23)$$

ω_c is the characteristic frequency employed to non dimensionalize δ_x and Y is surface tension and δf is expressed by

$$\omega_c = \frac{v}{R} \quad (24)$$

The non-dimensional excitation frequencies are given as

$$X_n = \frac{\omega}{\omega_{cn}} \quad (25)$$

$$X_w = \frac{\omega}{\omega_{cw}} \quad (26)$$

The subscripts w and n indicate wetting and nonwetting phases, respectively.

The frequency response is expressed as below (Hilpert (2007)).

$$\chi = \frac{\omega_c^2 \delta_x}{\delta f} \quad (27)$$

where

δf = Amplitude of the force applied

δ_x = Blob displacement

To estimate blob displacement, mass center of the blob is determined as given below (Hilpert (2007)):

$$z(t) = \frac{\iiint z\rho(x, y, z, t)dx dy dz}{\iiint \rho(x, y, z, t)dx dy dz} \quad (28)$$

First of all, the simulations are run to observe the behavior of the blob when excited with acoustic excitation. Following are the simulation parameters used for this case:

$$g_{zw} = 0.01$$

$$\delta f = 0.0001$$

$$\omega = 0.002$$

It can be observed from the Fig. 4 that the blob keeps oscillating about its initial position in a periodic manner. The magnitude of oscillation of the blob about its mean position depends on the frequency and the amplitude of force δf , geometry and surface wettability. Figure 4 shows the simulated blob after acoustic excitation. Contour plot in Fig. 4 shows that the blob oscillates when exposed to acoustic excitation. It is seen that the meniscus follows the flow by changing its radius of curvature (Hilpert et al. (2000)). The deformation of meniscus depends on the blob volume (ΔV) and nature of contact line motion. In some cases, the contact line adheres to surface and retains its contact microscopically for certain value of ΔV after contact line slides over the surface.

4.2. Frequency response behavior of blob

Figure 5 shows the response of the blob subjected to an oscillating body force $F_{3k} = \delta f(t) = \delta f \sin(\omega t)$, where the ω denotes excitation frequency which ranges from 0 to 1.5 ω_0 . The amplitude of applied oscillating force is $\delta f = 0.00005$. The lengths of the nonwetting phase and wetting phase are 60 and 40, respectively. The χ values are evaluated from Eq. (27). The temporal response for a given excitation $\delta f(t)$ can be found from the frequency response $\chi(\omega)$. The trend between the simulation results and that of Hilpert (2007) agrees well, nevertheless the present study is done for 3-D geometry. Hilpert (2007) has carried out LB simulation for two dimensional domain. The resonant frequency obtained is very close to the estimation done by Eq. (22) given by Hilpert (2007). The difference between the magnitude of displacement δ_x and frequency response χ of our results and that of Hilpert (2007) is due to the magnitude of force and the geometry they used.

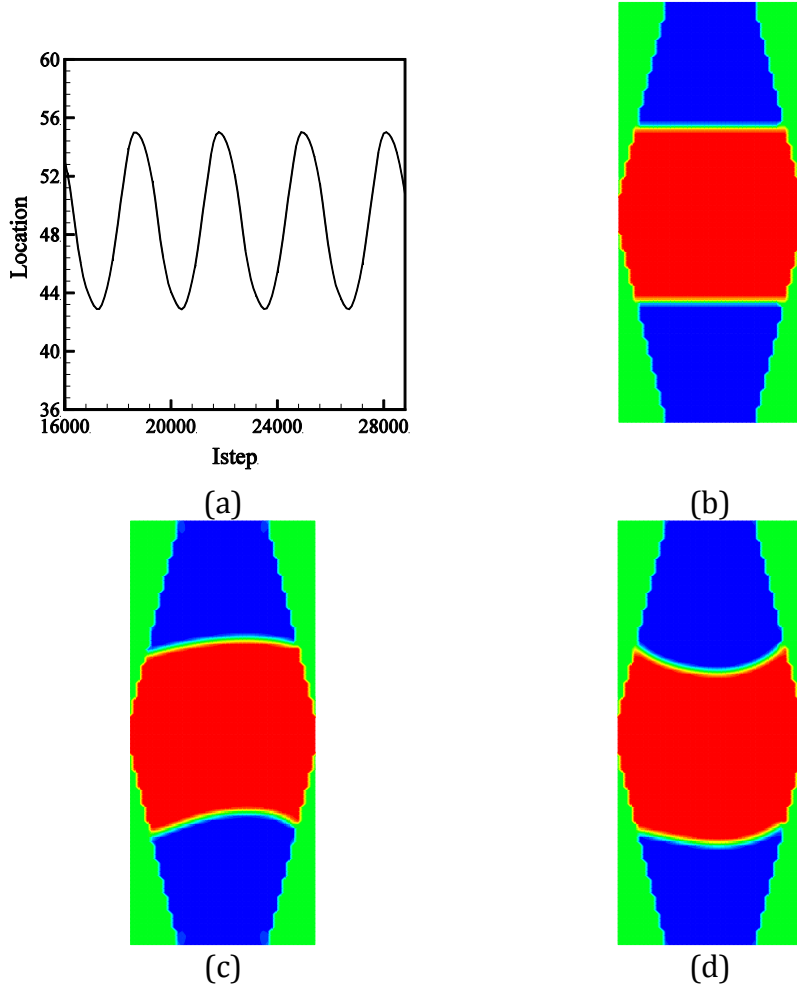


Figure 4: Excitation of a blob about pinned contact lines in a converging-diverging channel by an oscillatory force: (a) Behavior of a meniscus, (b)-(d) Three snapshots of the blob.

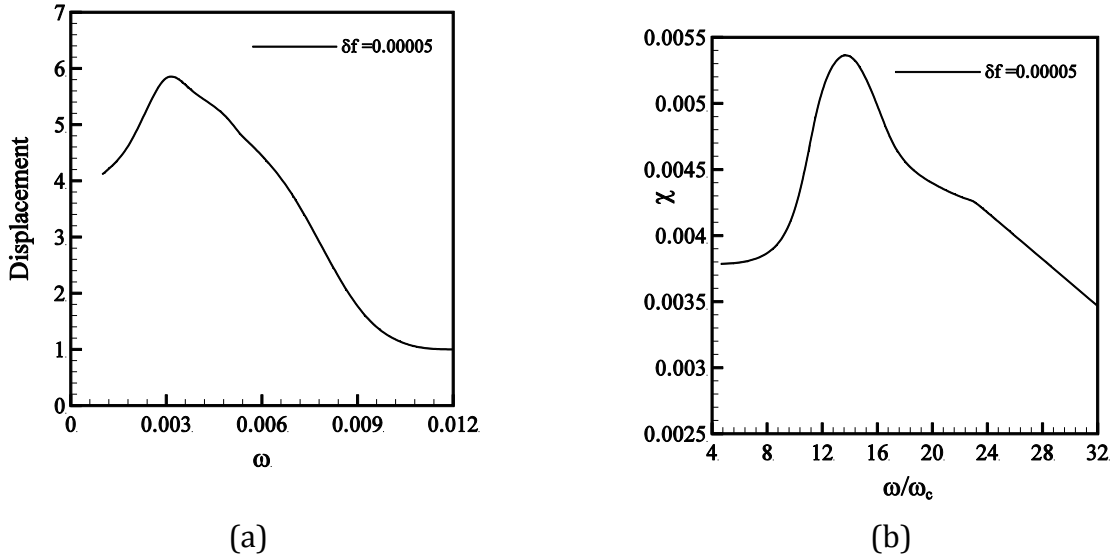


Figure 5: Effect of frequency: (a) change of displacement, (b) response of the blob.

The characteristic frequency ω_c determined from Eq. (24) is 0.00021. It can be seen that for resonant frequency $\omega = \omega_0 = 0.003$, the mean displacement reaches its maxima. The non-dimensional resonant frequency X_0 is 23.37 for $g_{2w} = 0.0$. The displacement of the blob decreases and becomes steady at high frequencies for the frequencies greater than resonance frequency. As discussed earlier, the nature of geometry also affects the extent of displacement. Figure 6 depicts the blob displacement plotted for a range of frequencies for the same oscillating excitation.

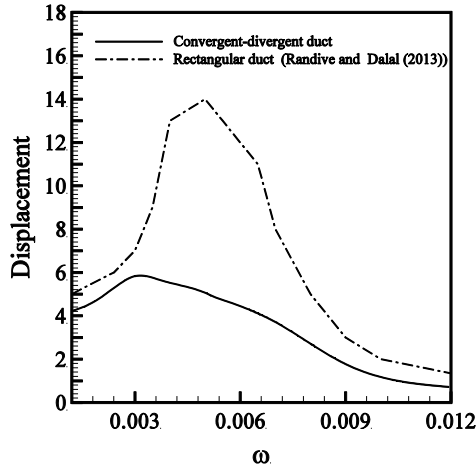


Figure 6: Effect of frequency in case of rectangular and convergent-divergent duct.

Although, the comparison cannot be done for the dynamics of blob in rectangular duct and convergent-divergent duct, it can be concluded that the displacement in case of convergent-divergent duct is overall lower. This is because of the more opportunities of trapping of the blob available due to cross-section of duct.

4.3. Mobilization of trapped blobs

Irregular geometry provides greater opportunities so as to trap the blob than the regular-shaped ones. This influences the dynamics of the blob, especially in network of pores. Hence, it is necessary to get insight into the physics behind the dynamics of trapped blob. Hence, the present work is about investigation on dynamics of trapped blob when exposed to capillarity induced resonance convergent-divergent duct.

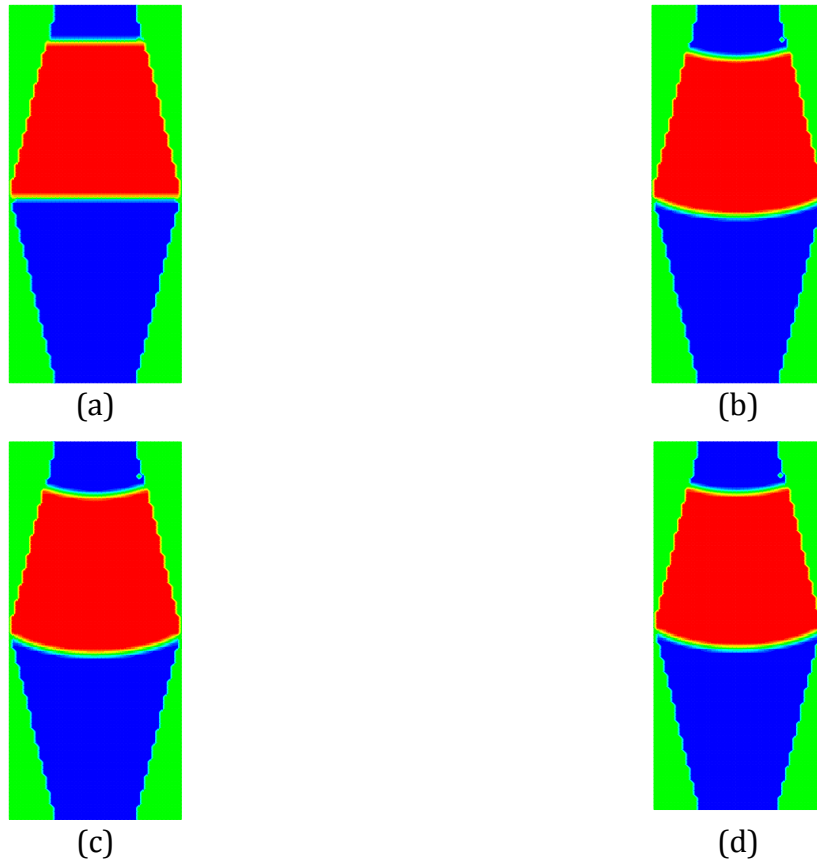


Figure 7: Snapshots of the blob at $\omega = 0.001$: (a) time step = 0, (b) time step = 7500, (c) time step = 10000, (d) time step = 13500.

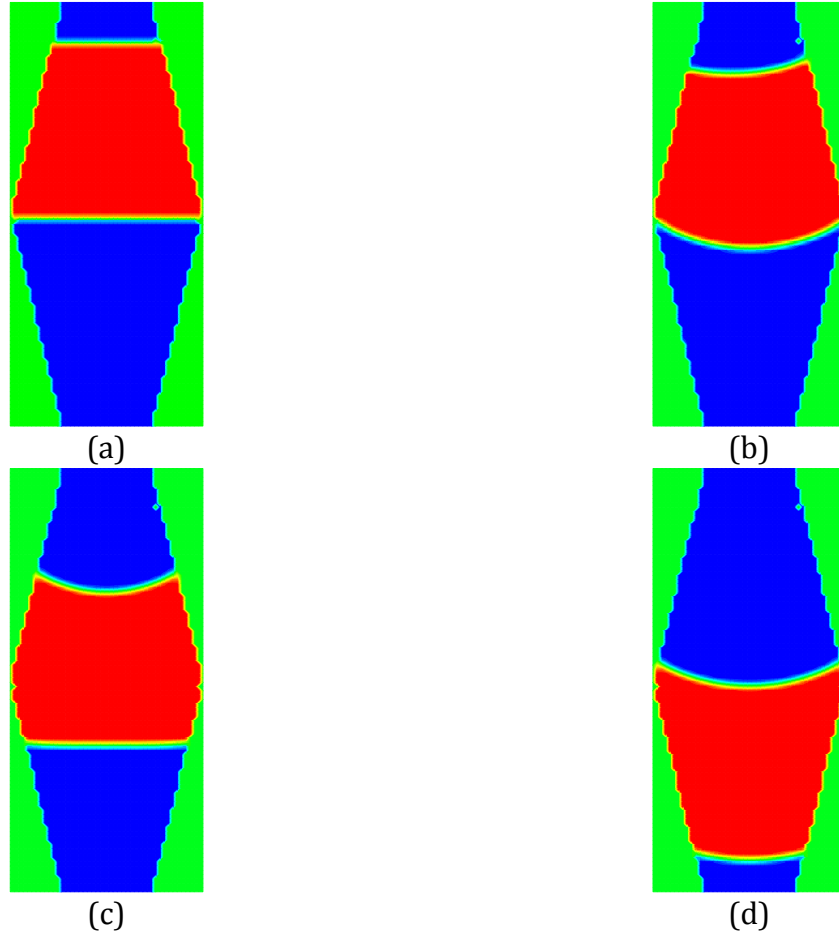


Figure 8: Snapshots of mobilized blob at $\omega = 0.003$: (a) time step = 0, (b) time step = 7500, (c) time step = 10000, (d) time step = 13500.

Initially, the numerical experiments are performed to find out the frequency at which the blob shows its maximum response. Figure 7 (a) shows the blob when excited with acoustic excitation, $\delta f = \sin(\omega t)$ for different frequencies. Peak displacement of the blob is observed at around $\omega_{\max} = 0.003$. Then, the blob is excited at a range of frequencies ranging from 0 to $1.5 \omega_{\max}$ with a body force (f_0) given by $f(t) = f_0 + f \sin(\omega t)$. It may be noted that amplitude δf is varied to mobilize the blob for a few excitation frequencies ω is near to ω_{\max} . It can be seen that the mobilization has taken place for $f_0 = 0.000046$ and $\delta f = 0.000006$. Figure 7 shows the snapshots of the blob at steady state for the frequency at which there is no mobilization has occurred whereas Fig. 8 shows the snapshots at the maximum excitation frequency when the mobilization has taken place. At frequency $\omega = 0.001$, the head meniscus travels past the throat although, the blob gets trapped owing to entrapment of the bottom meniscus (undergoing imbibition) has been restricted in a wide portion of the pore space (i.e., pore body). Excitation of the blob at $\omega = 0.003$, which is close to ω_0 , causes blob mobilization whereas excitation at $\omega = 0.001$, which is well below the resonant frequency ω_{\max} , leads to oscillation of the blob around the equilibrium state (see Fig. 9).

To quantify the extent of mobilization, the mean blob position is expressed as the time-averaged value of $z(t)$ of the last excitation cycle, z for all values of ω as shown in Fig. 9 (c). The filled symbol shows mobilization. The frequency response χ of the blob is very high consistent with earlier

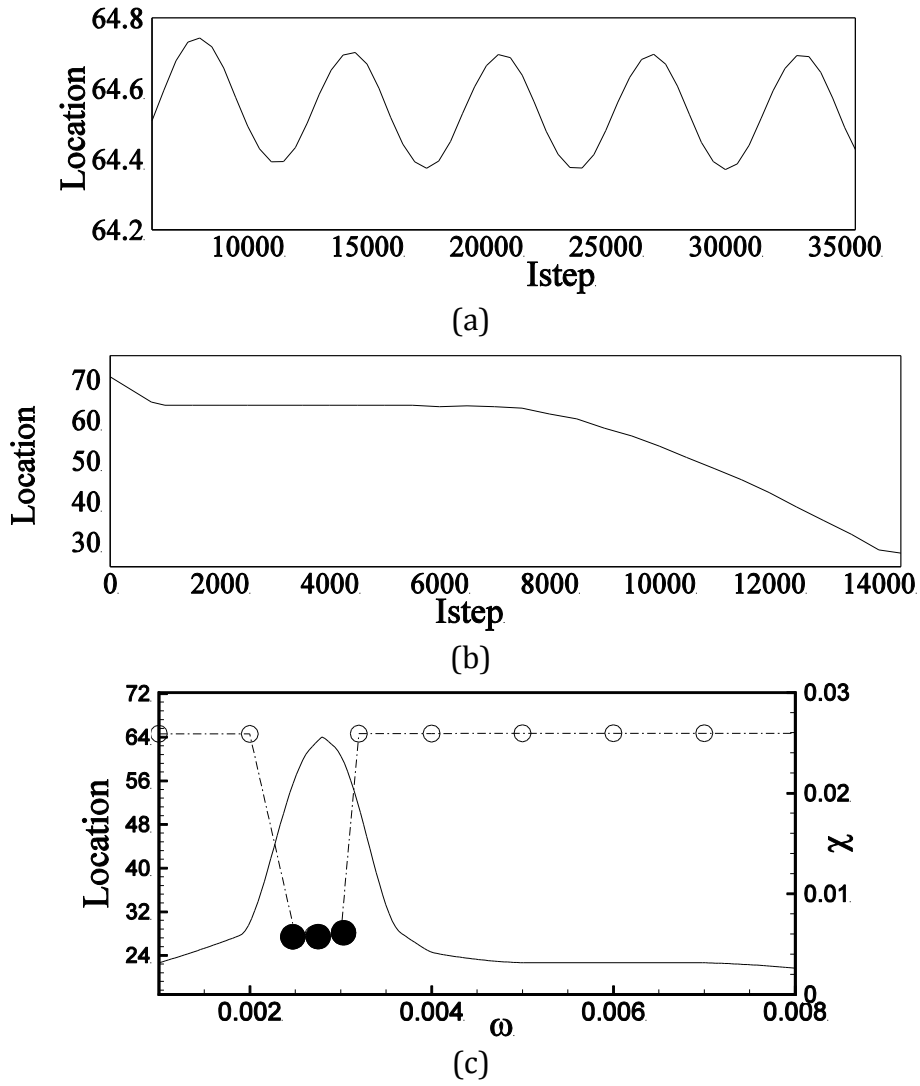


Figure 9: Mobilization of a blob in a convergent-divergent channel: (a) excitation at $\omega = 0.001$, (b) $\omega = 0.003$, (c) mean blob position during the last excitation cycle at various values of ω .

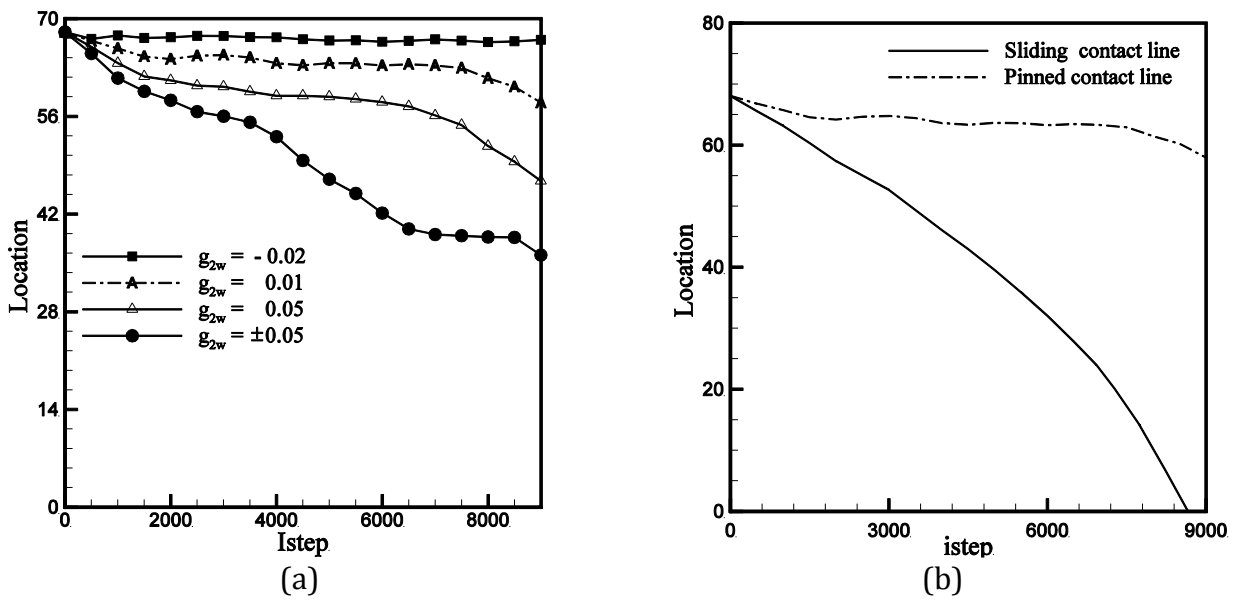


Figure 10: Effect of wettability on mobilization of the blob for $\omega = 0.003$.

observation at ω near to ω_{\max} . We can observe that the blob has moved to a significant length at a frequency close to ω_{\max} and the blobs trailing meniscus pass the pore body. It is interesting to note that the mobilization occurs only for a few excitation frequencies ($\omega = 0.0026$ and $\omega = 0.003$) which are close to ω_{\max} . The blob is moved by around 48 lattice units. Also, it can be seen that mobilization of the blob has only occurred for a few frequencies, which are very near to ω_{\max} .

These results show similar trends as that of earlier reported work of Hilpert (2007) which is done for two-dimensional domain. We have attempted to know how the wettability affects the mobilization at resonance frequency in particular. Trapped blob is positioned at the same location as shown in Fig. 7 (a) and mobilization of the blob is observed for different wettability scenarios. It is found that mobilization for unpinned blob is more since less resistance is experienced as compared to that of pinned blob (see Fig. 10 (a)). Also, the blob shows faster mobilization on hydrophobic surfaces ($g_{2w} = 0.05$) as compared to hydrophilic surface ($g_{2w} = -0.02$) (see Fig. 10 (b)). This is expected since the wetting tendency of hydrophilic surface poses difficulties for the blob to move and pass the constriction. This result suggests that capillarity induced resonance can be effective for achieving mobilization of the blob if wettability is taken into consideration.

5. Conclusions

The mechanism of capillarity-wettability interaction is explored to understand the behavior of the trapped blob. The blob response in converging-diverging channel subjected to an oscillatory force is systematically evaluated. It can be inferred from the LB simulations that trapped mobilization of trapped blob can be achieved using capillarity-induced resonance. The frequency response behavior of the blob shows quiet similar trend as that of earlier mobilization experiments reported in literature. Also, the role of wettability on the mobilization of the blob is analyzed. It can be concluded that the displacement of the blob reduces for the surfaces with mixed wettability as evident from relatively lesser displacement compared to with uniformly wettable surface. Further, it is seen that the excitation of the blob close to resonant frequency leads to a peak displacement of the blob. This study reveals that the extent of displacement is less than that for the same oscillating force as compared to the rectangular duct. This can be justified due to more number of entrapment opportunities in the case of convergent-divergent cross section. Therefore, use of resonance frequency in such configurations can be crucial in obtaining large displacement of the blob. It can be summarized that an optimal excitation of the blob depends on the surface wettability and frequency of excitation which could be useful significantly in dynamics of nonwetting phase trapped in channels.

References

- 1) Adroher, X. C., Wang, Y., (2011). Ex-situ and modeling study of two-phase flow in a single channel of polymer electrolyte membrane fuel cells. *J. Power Sources* 196, 9544–9551.
- 2) Amili, P., Yortsos, Y., (2006). Darcian dynamics: A new approach to the mobilization of a trapped phase in porous media. *Trans. Porous Media* 64, 25–49.
- 3) Beresnev, I., Johnson, A., (1994). Elastic-wave stimulation of oil production: a review of methods and results. *Geophysics* 59 (6), 1000–1017.
- 4) Briant, A. J., Wagner, A. J., Yeomans, J. M., (2004). Lattice Boltzmann simulations of contact line motion. i. liquid-gas systems. *Phys. Rev. E* 69, 031602–031614.
- 5) Chen, S., Doolen, G., (1998). Lattice Boltzmann method for fluid flows. *Annu. Rev. Fluid Mech.* 30, 329–364.
- 6) Davies, J., Maynes, D., Woolford, B., Webb, B. W., (2006). Laminar flow in a microchannel with superhydrophobic walls exhibiting transverse ribs. *Phys. of Fluids* 18, 087110 (1–11).
- 7) de Gennes, P. G., (1985). Wetting: Statics and dynamics. *Rev. Mod. Phys.* 57 (3), 827 – 863.
- 8) Dias, M., Payatakes, A., (1986). Network models for two-phase flow in porous media. ii: Motion of oil ganglia. *J. Fluid Mech* 164, 337–358.
- 9) Dullien, F. A. L., 1992. *Porous Media: Fluid Transport and Pore Structure*. Academic Press, San Diego, CA.

- 10) Graham, D. R., Higdon, J. J. L., (2000). Oscillatory flow of droplets in capillary tubes. part 1. straight tubes. *J. Fluid Mech.* 425, 31–53.
- 11) Gunstensen, A. K., Rothman, D. H., Zaleski, S., Zanetti, G., (1991). Lattice Boltzmann model of immiscible fluids. *Phys. Rev. A* 43, 4320–4327.
- 12) He, Q., Kasagi, N., (2008). Phase-field simulation of small capillary-number two-phase flow in a microtube. *Fluid Dynamics Research* 40 (7-8), 497–509.
- 13) He, X. Y., Chen, S. Y., Zhang, R. Y., (1999). A lattice Boltzmann scheme for incompressible multiphase flow and its application in simulation of Rayleigh-Taylor instability. *J. Comp. Phys.* 152, 642–663.
- 14) Hilpert, M., (2007). Capillarity-induced resonance of blobs in porous media: analytical solutions: lattice-Boltzmann modeling, and blob mobilization. *Journal of Colloid and Interface Science* 309, 493–504.
- 15) Hilpert, M., Jirka, G. H., Plate, E., (2000). Capillarity-induced resonance of oil blobs in capillary tubes and porous media. *Journal of Geophysics* 65, 874–883.
- 16) Hilpert, M., Stopper, D., Jirka, G. H., (1999). Resonance of a liquid column in a capillary tube. *Z. angew. Math. Phys.* 48, 424–438.
- 17) Hunt, J. R., Sitar, N., Udell, K. S., (1988). Nonaqueous phase liquid transport and cleanup: 1. analysis of mechanisms. *Water Resour. Res.* 24 (8), 1247–1258.
- 18) Iassonov, P. P., Beresnev, I. A., (2003). A model for enhanced fluid percolation in porous media by application of low-frequency elastic waves. *J. Geophys. Res.* 108, 2138–2146.
- 19) Inamuro, T., (2006). Lattice Boltzmann methods for viscous fluid flows and for two-phase fluid flows. *Fluid Dynamics Research* 38 (9), 641–659.
- 20) Kang, Q., Wang, M., Mukherjee, P. P., Lichtner, P. C., (2010). Mesoscopic modeling of multiphysicochemical transport phenomena in porous media. *Advances in Mechanical Engineering* 2, 142879.
- 21) Kang, Q., Zhang, D., Chen, S., (2002). Displacement of a two dimensional immiscible droplet in a channel. *Phys. of Fluids* 40, 3203–3214.
- 22) Kang, Q., Zhang, D., Chen, S., (2005). Displacement of a two dimensional immiscible droplet in a channel. *J. Fluid Mech* 545, 41–66.
- 23) Karapetsas, G., Sahu, K. C., Matar, O. K., (2013). Effect of contact line dynamics on the thermocapillary motion of a droplet on an inclined plate. *Langmuir* 29 (28), 8892–8906.
- 24) Karapetsas, G., Sahu, K. C., Sefiane, K., Matar, O. K., (2014). Thermocapillary-driven motion of a sessile drop: effect of non-monotonic dependence of surface tension on temperature. *Langmuir* 30 (15), 4310–4321.
- 25) Kostrov, S., Wooden, W., Roberts, P., (2001). In situ seismic shockwaves stimulate oil production. *Oil and Gas Journal* 99 (36), 47–52.
- 26) Larson, R., Davis, H., Scriven, L., (1981). Displacement of residual nonwetting fluid from porous media. *Chem. Eng. Sci.* 36 (1), 75–85.
- 27) Latt, J., (2007). Hydrodynamic limit of lattice Boltzmann equation. Ph.D. thesis University of Geneva.
- 28) Lauga, E., Stone, H. A., (2003). Effective slip in pressure-driven stokes flow. *J. Fluid Mech.* 489, 55–77.
- 29) Leger, L., Joanny, J. F., (1992). Liquid spreading. *Rep. Prog. Phys.* 55, 431–486. Martys, N. S., Chen, H., 1996. Simulation of multicomponent fluids in complex three-dimensional geometries by the lattice Boltzmann method. *Phys. Rev. E* 53, 743–750.
- 30) Mason, G., (1983). Mobilisation of oil blobs in the pore space of a random sphere packing. *Chem. Eng. Sci.* 38 (9), 1455–1460.

- 31) Mavko, G., Nur, A., (1979). Wave attenuation in partially saturated rocks. *Geophysics* 44, 161–178.
- 32) Mukherjee, P., (2007). Pore-scale modeling and analysis of the polymer electrolyte fuel cell catalyst layer. Ph.D Thesis Department of Mechanical Engineering Pennsylvania State University, USA.
- 33) Mukherjee, P. P., Kang, Q., Wang, C., (2011). Pore-scale modeling of two-phase transport in polymer electrolyte fuel cells-progress and perspective. *Energy Environ. Sci.* 4, 346–369.
- 34) Mukherjee, P. P., Wang, C., Kang, Q., (2009). Mesoscopic modeling of two-phase behavior and flooding phenomena in polymer electrolyte fuel cells. *Electrochim. Acta* 54, 6861–6875.
- 35) Murphy, W. F., (1982). Effects of partial water saturation on attenuation in massilon sandstone and vycor porous glass. *J. Acoust. Soc. Am.* 71 (6), 1458–1468.
- 36) Ng, K. M., Davis, H., Scriven, L., (1978). Visualization of blob mechanics in flow through porous media. *Chem. Eng. Sci.* 33 (8), 1009–1017.
- 37) Palan, P., Shepard, W. S., Williams, K. A., (2006). Removal of excess product water in a pem fuel cell stack by vibrational and acoustical methods. *J. Power Sources* 161, 1116–1125.
- 38) Palmer, I. D., Traviolia, M. L., (1980). Attenuation by squirt flow in undersaturated gas sands. *Geophysics* 45, 1780–1792.
- 39) Raabe, D., (2004). Overview of the lattice Boltzmann method for nano and microscale fluid dynamics in materials science and engineering. *Simul. Mater.Sci. Eng.* 12, 13–46.
- 40) Randive, P., Dalal, A., (2013). Capillarity induced resonance of blobs in a 3-D duct: lattice Boltzmann modelling. *Int. J. Heat Mass Transfer* 65, 635–648.
- 41) Roberts, P., Esipov, L., Majer, E., (2003). Elastic wave stimulation of oil reservoirs: Promising EOR technology? *The Leading Edge* 22 (5), 448–453.
- 42) Santos, J. E., Corbero, J. M., Douglas, J., (1990). Static and dynamic behavior of a porous solid saturated by a two-phase fluid. *J. Acoust. Soc. Am.* 87, 1428–1438.
- 43) Shan, X., Chen, H., Prasad, P. L. N., Basu, S., (1993). Lattice Boltzmann model for simulating flows with multiple phases and components. *Phys. Rev. E* 47, 1815–1817.
- 44) Shan, X., Doolen, G., (1995). Multicomponent lattice-Boltzmann model with interparticle interaction. *J. Stat. Phys.* 81 (4), 379–393.
- 45) Shan, X., Doolen, G. D., (1996). Diffusion in a multicomponent lattice Boltzmann equation model. *Phys. Rev. E* 54, 3614–3620.
- 46) Shina, J., Kima, H. J., (2013). Effect of confinement on droplet deformation in shear flow. *Int. J. Comput. Fluid Dyn.* 27 (8), 317–331.
- 47) Soares, E. J., Carvalho, M. S., Mendes, P. R. S., (2005). Immiscible liquid-liquid displacement in capillary tubes. *J. Fluids Eng.* 127 (1), 24–31.
- 48) Swift, M., Osborn, W., Yeomans, J., (1995). Lattice Boltzmann simulation of nonideal fluids. *Phys. Rev. Lett.* 75, 830–833.
- 49) Tuncay., K., Corapcioglu, M. Y., (1996). Body waves in poroelastic media saturated by two immiscible fluids. *J. Geophys. Res.* 101 (3), 25149–25159.
- 50) Wang, J., Dong, M., (2011). Trapping of the nonwetting phase in an interacting triangular tube bundle model. *Chem. Eng. Sci.* 66, 250–259.
- 51) Yadav, G. D., Mason, G., (1983). The onset of blob motion in a random sphere packing caused by flow of the surrounding liquid. *Chem. Eng. Sci.* 38 (9), 1451–1465.

- 52) Yiotis, A., Kainourgiakis, M., Kikkinides, E., Stubos, A., (2010). Application of the lattice-Boltzmann method to the modeling of population blob dynamics in 2d porous domains. *Comput. Math. Appl.* 59, 2315–2325.
- 53) Yiotis, A. G., Talon, L., Salin, D., (2013). Blob population dynamics during immiscible two-phase flows in reconstructed porous media. *Phy. Rev. E* 87, 033001–12.
- 54) Zhang, J., Kwok, D. Y., (2004). Lattice Boltzmann study on the contact angle and contact line dynamics of liquid-vapor interfaces. *Langmuir* 20, 8137–8141.